

LETTERS

Sound velocities of majorite garnet and the composition of the mantle transition region

T. Irifune¹, Y. Higo^{1,2}, T. Inoue¹, Y. Kono¹, H. Ohfuji¹ & K. Funakoshi²

The composition of the mantle transition region, characterized by anomalous seismic-wave velocity and density changes at depths of ~400 to 700 km, has remained controversial. Some have proposed that the mantle transition region has an olivine-rich 'pyrolite' composition^{1,2}, whereas others have inferred that it is characterized by pyroxene- and garnet-rich compositions ('piclogite'), because the sound velocities in pyrolite estimated from laboratory data are substantially higher than those seismologically observed^{3–5}. Although the velocities of the olivine polymorphs at these pressures (wadsleyite and ringwoodite) have been well documented, those of majorite (another significant high-pressure phase in the mantle transition region) with realistic mantle compositions have never been measured. Here we use combined *in situ* X-ray and ultrasonic measurements under the pressure and temperature conditions of the mantle transition region to show that majorite in a pyrolite composition has sound velocities substantially lower than those of earlier estimates, owing to strong non-linear decreases at high temperature, particularly for shear-wave velocity. We found that pyrolite yields seismic velocities more consistent with typical seismological models than those of piclogite in the upper to middle parts of the region, except for the potentially larger velocity jumps in pyrolite relative to those observed at a depth of 410 km. In contrast, both of these compositions lead to significantly low shear-wave velocities in the lower part of the region, suggesting possible subadiabatic temperatures or the existence of a layer of harzburgite-rich material supplied by the subducted slabs stagnant at these depths.

It has been accepted that the upper mantle is composed of peridotite or pyrolite compositions with about 60% olivine and lesser amounts of pyroxenes (~30%) plus a small but significant (~10%) amount of Al-rich phases, such as spinel and garnet, depending on pressure¹. Olivine transforms to wadsleyite at a pressure of ~13.5 GPa, and then to ringwoodite at ~18 GPa and decomposes to an assemblage of MgSiO₃-rich perovskite and (Mg,Fe)O rocksalt at ~24 GPa. In contrast, pyroxene progressively transforms to garnet structure with increasing pressure, forming an Al-deficient garnet (majorite) at pressures above ~16 GPa (ref. 6). Therefore, the mantle transition region (MTR) at depths between 410 km (~13.5 GPa) and 660 km (~24 GPa) is believed to be mainly composed of high-pressure forms of olivine and majorite, although small amounts of clinopyroxene and CaSiO₃-rich perovskite may be present at shallower and deeper regions of MTR, respectively^{6–8}.

Laboratory sound velocity measurements, however, have demonstrated that the velocities of wadsleyite (and ringwoodite) are substantially higher than those of olivine⁵, yielding unacceptably large velocity contrasts across the 410-km seismic discontinuity and also velocities too high to match seismological models in pyrolite composition for the upper to middle parts of the MTR. In contrast, majorite has been shown to exhibit lower velocities relative to

wadsleyite and ringwoodite^{9–12}, and provides better fits to seismological models if the proportion of olivine is reduced to 30–40%. So piclogite has been thought to yield velocities more consistent with those observed seismologically, although the uncertainty in laboratory measurements of the sound velocities has hindered firm conclusions^{5,13–16} because none of these measurements has been made under MTR conditions. We recently expanded the pressure and temperature conditions for combined *in situ* X-ray and ultrasonic measurements towards those of the MTR¹⁷. Here we applied this method to majorite with a 'pyrolite minus olivine' composition⁶ to address the chemical composition of MTR by combining the results on well-defined sound velocities of ringwoodite^{17–20}.

We conducted *in situ* X-ray and ultrasonic measurements under the pressure and temperature conditions of the MTR (Fig. 1a). Figure 1b shows a transmission electron microscope (TEM) image of the recovered sample after the run, showing that well-sintered and equilibrium textures formed, but no secondary phases, including no metallic iron. In contrast, we were unable to see any notable textural features on the polished sample using a scanning electron microscope (SEM), because the sample was fairly homogeneous and well-sintered with very small (<500 nm) grains. Powder X-ray diffraction measurement at the ambient condition for the sample demonstrated that all of the observed diffraction lines correspond to those of majorite (Supplementary Fig. 1), yielding lattice parameter $a = 11.580(1) \text{ \AA}$, which is almost the same as the value before the ultrasonic run ($a = 11.582(1) \text{ \AA}$). We note that a substantial decrease in lattice parameter is expected to occur if the majorite partially transforms to the low-pressure phase (clinopyroxene) or to the high-pressure phase (CaSiO₃-rich perovskite)⁶.

Figure 1c and d and Supplementary Table 1 show the sound velocity changes in the present majorite with increasing pressure and temperature. Both the P- and S-wave velocities v_p and v_s increase with increasing pressure and decrease with increasing temperature, whereas the temperature effect on v_s is so large that at the highest pressure (~18 GPa) and temperature (1,673 K), v_s is substantially lower than at the ambient condition. Also, the rates of the velocity decreases in both v_p and v_s become more prominent at higher temperatures. A similar but less obvious nonlinear temperature dependence was also observed for (Mg,Fe)₂SiO₄ ringwoodite under corresponding pressure and temperature conditions¹⁷.

Unit-cell volume changes of majorite with pressure and temperature are determined on the basis of *in situ* X-ray diffraction measurements. The X-ray density of majorite at each pressure and temperature can be determined by the volume data combined with the chemical composition of majorite (Fig. 1e and Supplementary Table 1), yielding a zero-pressure density of $\rho_0 = 3.605(1) \text{ g cm}^{-3}$, which is in good agreement with the earlier result by quenched method ($\rho_0 = 3.61 \text{ g cm}^{-3}$) (ref. 6). The isothermal bulk modulus derived from the compression data at room temperature

¹Geodynamics Research Center, Ehime University, Matsuyama 790-8577, Japan. ²Japan Synchrotron Research Institute, Hyogo 679-5198, Japan.

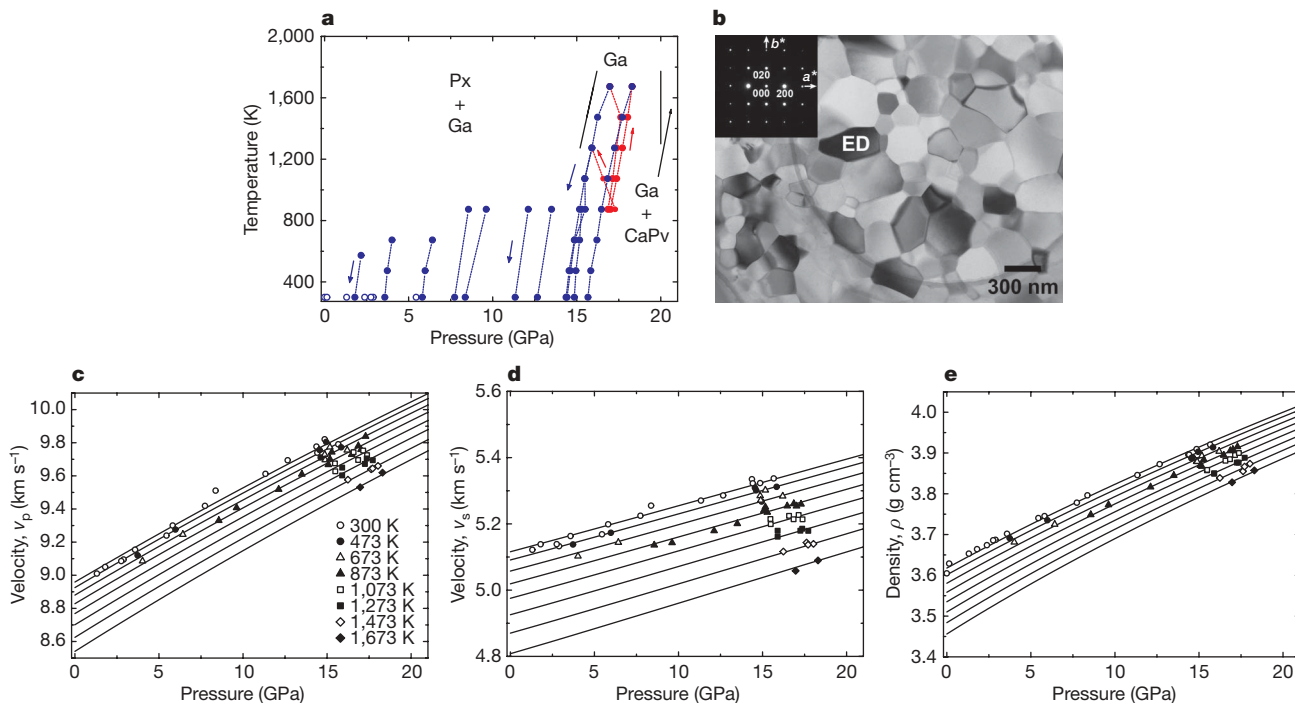


Figure 1 | Experimental conditions and results of the combined ultrasonic and *in situ* X-ray measurements on a polycrystalline majorite sample with pyrolite minus olivine composition. **a**, Pressure–temperature conditions of the combined *in situ* X-ray and ultrasonic measurements. The measurements were mostly made while decreasing temperature (blue), but some measurements in the stability field of majorite were made while increasing temperature (red). The open circles represent pressures where the measurements were made without heating the sample upon compression. Phase boundaries are based on a phase equilibrium study⁶.

b, A TEM image of the sample recovered from the sound velocity measurements at high pressure and high temperature. The inset is a selected area electron diffraction pattern from the grain marked ED—a single crystal of majorite garnet. No evidence for the presence of other phases is obtained, and the crystals exhibit an equilibrium texture with grain sizes of typically 200–300 nm. **c–e**, P-wave velocity (**c**), S-wave velocity (**d**) and density (**e**) changes of majorite with pressure and temperature.

($K_{T0} = 162(1)$ GPa, assuming $K_{T0}' = 4.2$) is consistent with the bulk modulus $K_{S0} = 164.4(5)$ GPa based on the ultrasonic measurements.

By a linear fitting of the longitudinal and shear moduli derived from the velocity data combined with the X-ray density data, we obtained the bulk and shear moduli K_0 and G_0 and their pressure and temperature derivatives (Table 1), which are in general comparable to those obtained for majorite with a composition of 50% $MgSiO_3$ and 50% $Mg_3Al_2Si_3O_{12}$ ($En_{50}Py_{50}$), using the Brillouin scattering method^{11,12}, although the dG/dP and dG/dT values we obtained are smaller. We also obtained the second temperature derivatives for our majorite by fitting a polynomial equation to the same data set, and calculated variations of the sound velocities with temperature at some pressures (16, 18 and 20 GPa) of the middle part of the MTR (Fig. 2). v_p and v_s and their temperature dependence in the present pyrolitic majorite are quite close to those of $En_{50}Py_{50}$ majorite at relatively low temperatures below $\sim 1,000$ K. However, these velocities, particularly v_s , based on the present data, exhibit a notable nonlinear decrease with temperature, as compared with those of $En_{50}Py_{50}$ majorite, which were extrapolated using the experimental data at relatively low ($< 1,073$ K) temperatures¹².

Majorite garnet is suggested to have a temperature dependence of less than half ($dv_p/dT = -1.6 \times 10^{-4} \text{ km s}^{-1} \text{ K}^{-1}$ and $dv_s/dT = -1.1 \times 10^{-4} \text{ km s}^{-1} \text{ K}^{-1}$) that of high-pressure forms of olivine ($dv_p/dT = -3.5 \times 10^{-4} \text{ km s}^{-1} \text{ K}^{-1}$ and $dv_s/dT = -3.8 \times 10^{-4} \text{ km s}^{-1} \text{ K}^{-1}$ for wadsleyite, $dv_p/dT = -3.0 \times 10^{-4} \text{ km s}^{-1} \text{ K}^{-1}$ and $dv_s/dT = -2.9 \times 10^{-4} \text{ km s}^{-1} \text{ K}^{-1}$ for ringwoodite) near the bottom of the MTR¹². We obtained similarly small negative values ($dv_p/dT = -1.5 \times 10^{-4} \text{ km s}^{-1} \text{ K}^{-1}$ and $dv_s/dT = -1.2 \times 10^{-4} \text{ km s}^{-1} \text{ K}^{-1}$) for our majorite from the low-temperature data at 18 GPa. However, because of the notable nonlinear nature of the temperature dependence, these temperature derivatives at high temperatures at this depth are calculated to be $dv_p/dT = -4.0 \times 10^{-4} \text{ km s}^{-1} \text{ K}^{-1}$ and $dv_s/dT = -3.1 \times 10^{-4} \text{ km s}^{-1} \text{ K}^{-1}$, which are similar to those of the high-pressure forms of olivine. Therefore we suggest that the temperature variations in the MTR inferred from the lateral velocity heterogeneity combined with the elastic properties of only high-pressure forms of olivine would not be affected by the presence of majorite, in spite of the earlier study based on the results at lower temperatures¹². The $R = \ln v_s / \ln v_p$ value²¹ for our majorite is 1.5 for all the present temperatures at 18 GPa, which is higher than those of

Table 1 | Elastic parameters of majorite

Composition	K_0 (GPa)	G_0 (GPa)	dK/dP	dG/dP	dK/dT (GPa K^{-1})	dG/dT (GPa K^{-1})	d^2K/dT^2 (GPa K^{-2})	d^2G/dT^2 (GPa K^{-2})	Reference
Pyrolite minus olivine	164.4(5)	94.9(2)	4.24(6)	1.11(3)	-0.0129(8)	-0.0103(4)	NA	NA	This study*
Pyrolite minus olivine	164.2(5)	94.7(2)	4.22(5)	1.08(2)	-0.0091(16)	-0.0074(5)	$-6(3) \times 10^{-6}$	$-5(1) \times 10^{-6}$	This study**
En38Py62	171(5)	90(1)	6.2(5)	1.9(2)	NA	NA	NA	NA	Ref. 10
En50Py50	167(3)	90(2)	NA	NA	-0.0145(20)	-0.0082(10)	NA	NA	Ref. 12
En50Py50	167(3)	90(2)	4.2(3)	1.4(2)	NA	NA	NA	NA	Ref. 11
En80Py20	163(3)	88(2)	NA	NA	-0.0143(20)	-0.0083(10)	NA	NA	Ref. 12

NA, not available. ***Linear and polynomial fits (including the second derivative of temperature $M = M_0 + dM/dP \times P + dM/dT \times (T - 300) + (1/2)d^2M/dT^2 \times (T - 300)^2$, where M represents the longitudinal and shear moduli, respectively).

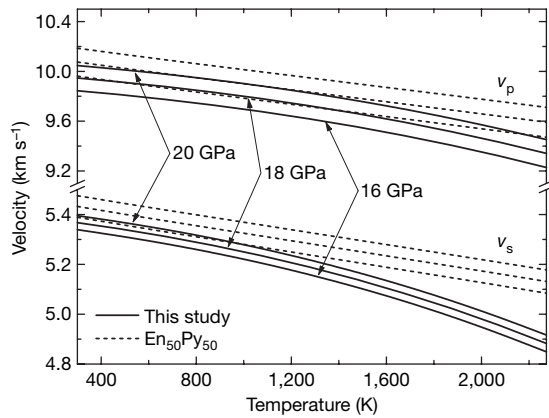


Figure 2 | Variations of sound velocities of majorite with temperature for the selected pressures in MTR. The solid lines show those derived from the present data, while the dotted lines are extrapolated using the elastic properties of majorite with a composition $\text{En}_{50}\text{Py}_{50}$, where En is MgSiO_3 and Py is $\text{Mg}_3\text{Al}_2\text{Si}_3\text{O}_{12}$ (ref. 12).

most high-pressure phases but is close to those seismologically constrained, whereas $d v_p/dP$ and $d v_s/dP$ are $0.049\text{--}0.052$ and $0.014\text{ km s}^{-1}\text{ GPa}^{-1}$ over the pressure range of the MTR.

We evaluated v_p and v_s for pyrolite and piclogite compositions, using elastic moduli and X-ray densities obtained for $(\text{Mg}_{0.91}\text{Fe}_{0.09})_2\text{SiO}_4$ ringwoodite¹⁷ and those of our majorite along a geotherm²² (Fig. 3). These velocities for the middle part of the MTR ($\sim 520\text{--}580$ km), where only ringwoodite and majorite coexist in both of these mantle compositions^{6,16}, are tightly constrained within $\sim 0.5\%$. We also estimated the velocity changes in pyrolite and piclogite in other regions of the MTR using our data and those of earlier studies on other high-pressure phases^{15,17,23} in conjunction with the phase proportion data^{6,7,16}. These calculations for the upper and lower parts of the MTR involve errors of $\sim 2\text{--}3\%$ owing to uncertainties in the mineral physics parameters.

For v_p , both pyrolite and piclogite compositions lead to the velocities consistent with those of the typical seismological models^{24,25} throughout the MTR. v_s for pyrolite also agrees well with those of the seismological models in the upper half to middle parts of MTR, whereas piclogite yields substantially lower v_s in these regions. It should be noted that pyrolite yields larger velocity jumps at 410 km discontinuity than do the seismological models and piclogite. A corresponding sound velocity measurement on wadsleyite at the relevant pressure and temperature conditions is needed to address this issue, because the velocities of wadsleyite at temperatures of MTR may be lower than those estimated earlier, which yield smaller velocity jumps in pyrolite, consistent with the seismological models.

For the lower part of the MTR, both pyrolite and piclogite fail to explain the seismological v_s models, mainly because of the unexpectedly low v_s of majorite. The progressive formation of CaSiO_3 -rich perovskite (which has high velocities) from the majorite phase may explain the discrepancy in these compositions, but direct measurement of this unquenchable phase under these pressure and temperature conditions is needed to confirm this.

There may be a low-temperature anomaly due to the presence of stagnant slabs near the 660 km depth²⁶, which should increase the average velocities in this region. The temperature dependence of the velocities for ringwoodite and majorite obtained in our study indicates that temperatures lower by about 400 K are required to match the seismological models. On the other hand, subducted slabs are generally assumed to be composed of a thin layer of oceanic crust underlain by a thicker residual harzburgite. This harzburgite should have olivine content and an $\text{Mg}/(\text{Mg}+\text{Fe})$ value substantially higher than those of the surrounding mantle, both of which increase the seismic velocities. Thus a combination of relatively low temperatures and the Mg- and olivine-rich nature of the stagnant slab may explain the apparent

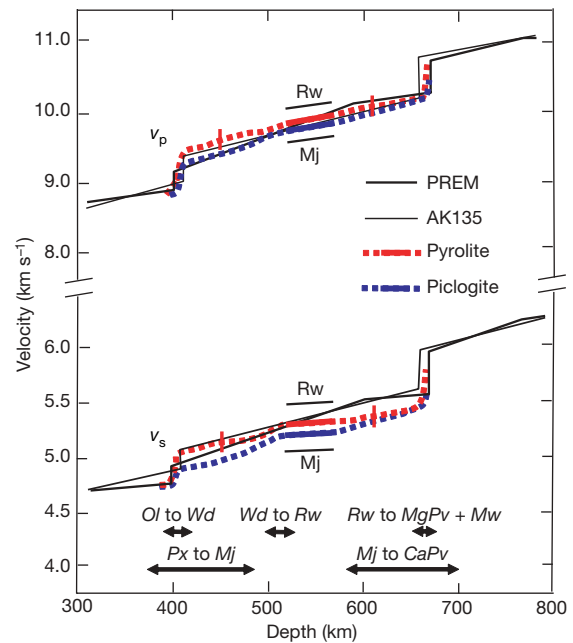


Figure 3 | A comparison of the sound velocities for pyrolite and piclogite compositions with representative seismological models in the MTR. Short black horizontal solid lines show the velocities of majorite (MJ, obtained in this study) and of ringwoodite (Rw, using the same method¹⁷). Thicker horizontal solid lines are for pyrolite (red) and piclogite (blue) calculated by combining these data and the mineral proportions defined by phase equilibrium studies^{6,16}. The dotted red and blue lines are the estimated velocity changes using a combination of the phase equilibrium data^{6–8,16} and the present and other elastic properties of relevant high-pressure phases^{15,17,23}. Vertical red bars show typical errors in the velocity calculation for the upper and lower parts of the MTR (those based on the present study for the middle part are nearly equivalent to the thickness of the solid bars). Arrows indicate the depths at which phase transitions in major minerals take place in pyrolite⁶. Ol = olivine; Wd = wadsleyite; Py = pyroxene; MgPv = MgSiO_3 perovskite; Mw = magnesio-wüstite. PREM and Ak135 are representative seismological models^{24,25}.

disagreement of the elastic velocities of pyrolite (and piclogite) and those of the seismological models in the lower part of the MTR.

METHODS

A polycrystalline sample of majorite with the ‘pyrolite minus olivine’ composition was synthesized using a multi-anvil apparatus at 18 GPa at 1,500 K under dry conditions. The hot-pressed rod sample was of pure majorite with grain sizes less than $\sim 0.2\text{ }\mu\text{m}$, and had a porosity of 0.5%. An electron microprobe analysis shows the sample to be homogeneous and to have composition $\text{SiO}_2 = 50.60$, $\text{TiO}_2 = 0.60$, $\text{Al}_2\text{O}_3 = 11.14$, $\text{Cr}_2\text{O}_3 = 0.97$, $\text{MgO} = 22.32$, $\text{CaO} = 9.33$, $\text{FeO} = 3.02$ and $\text{Na}_2\text{O} = 0.75$ (wt%), which is close to that reported in ref. 6.

Combined *in situ* X-ray and ultrasonic measurements were conducted using a 1,500-ton multianvil apparatus at SPring-8. The sample was surrounded by an NaCl sleeve and heated with a cylindrical platinum foil in a $(\text{Mg},\text{Co})\text{O}$ pressure medium. The pressure was monitored by unit-cell volumes of NaCl and Au in a pellet of a mixture of $\text{NaCl}+\text{Au}+\text{BN}$, placed adjacent to the sample, using equations of state^{27,28}. We used the NaCl scale as the primary pressure scale in the present analysis. The temperature was measured with a $\text{W}_{97}\text{Re}_3\text{--W}_{75}\text{Re}_{25}$ thermocouple, the hot junction of which was placed near the sample. The temperature uncertainty due to the gradient in the furnace and fluctuation of heating is within $\pm 2\%$ of the nominal value.

X-ray diffraction from the sample and the pressure markers was observed using an energy-dispersive system, and the sample length was measured with a high-resolution (1 pixel = $\sim 2\text{ }\mu\text{m}$) charge-coupled device (CCD) camera. Ultrasonic measurements were conducted while *in situ* X-ray observations were being made, and the travel times of both P- and S-waves were determined by a pulse–echo method using a transfer function technique²⁹. The data acquisition time at each pressure and temperature point was typically 10 min. The overall uncertainties of the present velocity measurements are within $\pm 0.5\%$ in both v_p and v_s .

Received 20 July; accepted 5 December 2007.

1. Ringwood, A. E. *Composition and Petrology of the Earth's Mantle* (McGraw-Hill, New York, 1975).
2. Bina, C. R. & Wood, B. J. The olivine-spinel transitions: experimental and thermodynamic constraints and implications for the nature of the 400 km seismic discontinuity. *J. Geophys. Res.* **92**, 4853–4866 (1987).
3. Anderson, D. L. & Bass, J. D. Transition region of the Earth's upper mantle. *Nature* **320**, 321–328 (1986).
4. Duffy, T. S., Zha, C. S., Downs, R. T. & Mao, H. K. Elasticity of forsterite up to 16 GPa. *Nature* **378**, 170–173 (1995).
5. Li, B., Liebermann, R. C. & Weidner, D. J. Elastic moduli of wadsleyite (β - Mg_2SiO_4) to 7 gigapascal and 873 Kelvin. *Science* **281**, 675–677 (1998).
6. Irifune, T. & Ringwood, A. E. in *High-Pressure Research in Mineral Physics* (eds Manghni, M. & Syono, Y.) 221–230 (Terra/American Geophysical Union, Tokyo/Washington, 1987).
7. Irifune, T. Absence of an aluminous phase in the upper part of the of the lower mantle. *Nature* **370**, 131–133 (1994).
8. Irifune, T. & Isshiki, M. Iron partitioning in a pyrolite mantle and nature of the 410-km seismic discontinuity. *Nature* **392**, 702–705 (1998).
9. Gwanmesia, G. D., Chen, G. & Liebermann, R. C. Sound velocities in MgSiO_3 -garnet to 8 GPa. *Geophys. Res. Lett.* **24**, 4553–4556 (1998).
10. Liu, J., Chen, G., Gwanmesia, G. D. & Liebermann, R. C. Elastic wave velocities of pyrope-majorite garnets ($\text{Py}_{62}\text{Mj}_{38}$ and $\text{Py}_{50}\text{Mj}_{50}$) to 9 GPa. *Phys. Earth Planet. Inter.* **120**, 153–163 (2000).
11. Sinogeikin, S. V. & Bass, J. D. Elasticity of majorite and a majorite-pyrope solid solution to high pressure: implications for the transition zone. *Geophys. Res. Lett.* **29**, doi:10.1029/2001GL013937 (2002).
12. Sinogeikin, S. V. & Bass, J. D. Elasticity of pyrope and majorite-pyrope solid solutions to high temperatures. *Earth Planet. Sci. Lett.* **203**, 549–555 (2002).
13. Ita, L. & Stixrude, L. Petrology, elasticity and composition of the mantle transition zone. *J. Geophys. Res.* **97**, 6849–6866 (1992).
14. Agee, C. B. Phase transformations and seismic structure in the upper mantle and transition zone. *Rev. Mineral.* **37**, 165–203 (1998).
15. Vacher, P., Mocquet, A. & Sotin, C. Computation of seismic profiles from mineral physics: the importance of the non-olivine components for explaining the 660 km depth discontinuity. *Phys. Earth Planet. Inter.* **106**, 275–298 (1998).
16. Nishihara, Y. & Takahashi, E. Phase relation and physical properties of an Al-depleted komatiite to 23 GPa. *Earth Planet. Sci. Lett.* **190**, 65–77 (2001).
17. Higo, Y., Inoue, T., Irifune, T., Funakoshi, K. & Li, B. Elastic wave velocities of $(\text{Mg}_{0.91}\text{Fe}_{0.09})_2\text{SiO}_4$ ringwoodite under P-T condition of the mantle transition region. *Phys. Earth Planet. Inter.* (in the press).
18. Li, B. Compressional and shear wave velocities of ringwoodite γ - Mg_2SiO_4 to 12 GPa. *Am. Mineral.* **88**, 1312–1317 (2003).
19. Higo, Y., Inoue, T., Li, B., Irifune, T. & Liebermann, R. C. The effect of iron on the elastic properties of ringwoodite at high pressure. *Phys. Earth Planet. Inter.* **159**, 276–285 (2006).
20. Sinogeikin, S. V., Bass, J. B. & Katsura, T. Single-crystal elasticity of ringwoodite to high pressure and high temperature: implication for 520 km seismic discontinuity. *Phys. Earth Planet. Inter.* **136**, 41–66 (2003).
21. Masters, G., Laske, G., Bolton, H. & Dziewonski, A. M. in *Earth's Deep Interior: Mineral Physics and Seismic Tomography From the Atomic to the Global Scale* (eds Karato, S., Forte, A. M., Liebermann, R. C., Masters, G., Stixrude, L.) 63–87 (AGU, Washington DC, 2000).
22. Akaogi, M., Ito, E. & Navrotsky, A. Olivine-modified spinel-spinel transitions in the system Mg_2SiO_4 - Fe_2SiO_4 : calorimetric measurements, thermochemical calculation, and geophysical application. *J. Geophys. Res.* **94**, 15671–15685 (1989).
23. Cammarano, F., Goes, S., Vacher, P. & Giardini, D. Inferring upper-mantle temperatures from seismic velocities. *Phys. Earth Planet. Inter.* **138**, 197–222 (2003).
24. Dziewonski, A. M. & Anderson, D. L. Preliminary reference Earth model. *Phys. Earth Planet. Inter.* **25**, 297–356 (1981).
25. Kennet, B. L. N., Engdahl, E. R. & Buland, R. Constraints on seismic velocities in the Earth from traveltimes. *Geophys. J. Int.* **122**, 108–124 (1995).
26. Fukao, Y., Widiyantoro, S. & Obayashi, M. Stagnant slabs in the upper and lower mantle transition region. *Rev. Geophys.* **39**, 291–323 (2001).
27. Anderson, O. L., Issak, D. G. & Yamamoto, S. Anharmonicity and the equation of state for gold. *J. Appl. Phys.* **65**, 1534–1543 (1989).
28. Decker, D. J. High-pressure equation of state for NaCl, KCl, and CsCl. *J. Appl. Phys.* **42**, 3239–3244 (1971).
29. Li, B., Kung, J. & Liebermann, R. C. Modern techniques in measuring elasticity of Earth materials at high pressure and high temperature using ultrasonic interferometry in conjunction with synchrotron X-ray radiation in multi-anvil apparatus. *Phys. Earth Planet. Inter.* **98**, 79–91 (2004).

Supplementary Information is linked to the online version of the paper at www.nature.com/nature.

Acknowledgements We thank B. Li, R. C. Liebermann, J. Kung, I. Jackson for their help and advice in ultrasonic techniques, T. Shinmei, A. Yamada, T. Kunimoto, Y. Tange, N. Nishiyama for their assistance in synchrotron experiments, and C. A. McCammon and I. Jackson for comments on the manuscript. This paper was written while T. Irifune was on leave at the Bayreuth Geoinstitute, and supported by the Humboldt Foundation. This study is based on a research proposal to SPring-8 with a Grant-in-Aid for Scientific Research from the Japanese government (to T. Irifune).

Author Contributions T. Irifune directed the research project and wrote the manuscript. Y.H. did most of the experiments and analyses of the data with the help of T. Inoue, Y.K. and K.F. The TEM and XRD analyses of the recovered sample were conducted by H.O. and T. Inoue, respectively. All authors discussed the results and commented on the manuscript.

Author Information Reprints and permissions information is available at www.nature.com/reprints. Correspondence and requests for materials should be addressed to T. Irifune (irifune@dpcehime-u.ac.jp).